

RESEARCH ARTICLE

OPEN ACCESS

## Growth and Characterization of BTCC Crystals Added with Urea

I. S. Prameela Kumari And C.K. Mahadevan

Physics Research Centre, S.T. Hindu College – 629 002, Tamil Nadu, India.

### ABSTRACT

Pure and impurity added (with urea) bis(thiourea)cadmium chloride (BTCC) single crystals were grown by the slow evaporation technique. The grown crystals were characterized by powder XRD analysis. Elemental analysis was made by energy dispersive X-ray analysis. The UV-VIS-NIR absorption spectra have shown that the grown doped crystals have wide optical transparency in the entire visible region and UV-cut of wavelengths are less than that for pure BTCC crystals. Second harmonic generation efficiency measurements carried out with different dopant concentrations reveal that the nonlinear optical property is enhanced by the addition of dopant. DC and AC electrical measurements were carried out on the pure and doped BTCC crystals at various temperatures ranging from 40-100°C. The present study also shows the variation of dielectric properties (dielectric constant, dielectric loss and AC conductivity) as a function of frequency and temperature for the grown crystals. Activation energies were also determined and reported.

**Keywords** - Crystals, Crystal growth, Electrical properties, Optical properties, Single crystals, X-ray diffraction

### I. Introduction

In the recent years efforts have been made to develop new inorganic, organic and semi-organic nonlinear optical (NLO) crystals. The organic NLO materials have large nonlinear optical co-efficient compared to inorganic material, but their use is impeded by their poor mechanical and thermal properties, low laser damage threshold, etc [1]. The pure inorganic materials have excellent mechanical and thermal properties but possess relatively modest optical nonlinearities due to lack of extended  $\pi$  electron delocalization [2]. In view of these problems, new types of hybrid NLO materials have been explored from organic and inorganic complexes called semi-organics [2, 3].

Nonlinear optical (NLO) materials have a significant impact on laser technology, optical communication and optical storage devices. Bis(thiourea)cadmium chloride (BTCC) is a potential NLO material crystal for various applications in the field of laser and optoelectronics [4-17]. The second harmonic generation (SHG) efficiency of BTCC is 0.73 times higher than urea [9]. It also possesses good mechanical properties which are comparable with KDP [10]. Another remarkable feature of BTCC is that it has a high laser damage threshold [4]. Several dopants have been found to affect the structural and physical properties of the host compound [18].

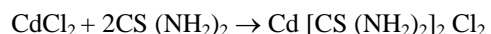
In the present investigation urea was considered in molar percent as dopant in saturated BTCC solution. It is expected to occupy interstitial positions if added as impurity. It is also expected to disturb the hydrogen bonding networks of BTCC, as urea is also a representative of hydrogen bonded material. Inorder to understand the effect of urea as an

impurity on the physical properties of BTCC crystals, in the present study, we have grown pure and urea doped BTCC single crystals and characterized structurally, optically and electrically.

### II. Experimental Details

#### 2.1 Growth of single crystals

Single crystals of BTCC were grown by using the procedure reported earlier [6]. Analytical reagent (AR) grade samples of the required chemicals (cadmium chloride, thiourea and urea) along with double distilled water were used. BTCC was synthesized from aqueous solutions of  $\text{CdCl}_2$  and thiourea in the ratio 1:2 following the chemical reaction.



The solution was heated and left for evaporation to dryness at room temperature. The purity of the synthesized salt was increased by successive re-crystallization process. Temperature as low as 48 °C was maintained in order to avoid decomposition. Crystal growth was carried out by the slow evaporation technique. To grow urea doped BTCC single crystals, urea was added with saturated solution of BTCC separately in five different BTCC: impurity molecular ratios, viz. 1:0.000 (pure BTCC), 1:0.0025, 1:0.0050, 1:0.0075 and 1:0.010. To understand the influence of dopants and to compare the crystalline perfections with undoped crystals both pure and doped crystals were grown under similar conditions. The period of growth of the crystals ranged from 20-25 days.

#### 2.2 Characterization

Powder X-ray diffraction (PXRD) data were collected by employing PANalytical diffractometer

with CuK<sub>α</sub> radiation ( $\lambda = 1.54056 \text{ \AA}$ ) scanned over 20 range of 10-80 °C at the rate of 1 °/min, to understand the crystallinity of the crystals grown. Lattice parameters for the pure BTCC crystal were determined by using an ENRAF NONIUS CAD-4 automatic X-ray diffractometer with MoK<sub>α</sub> radiation ( $\lambda = 0.71073 \text{ \AA}$ ). The PXRD data were indexed by following the procedures of Lipson and Steeple [19].

The incorporation of the dopant urea in the BTCC crystal lattice was verified by using energy dispersive X-ray analysis [EDAX] technique using a JOEL/EO-JSM 6390.

The UV-Vis-NIR absorption spectra were recorded for all the five grown crystals in the wavelength range 100-900 nm by using a SHIMADZU UV-1700 spectrophotometer with a medium scan speed sampling interval 0.5. The SHG efficiency of the grown crystals were checked using the powder SHG-technique developed by Kurtz and Perry [20]. The crystals were ground into powder and densely packed in between two glass slides. Nd: YAG laser beam of wavelength 1064 nm was made to fall normally on the sample cell. The emission of green light (wavelength 532 nm) confirms the SHG of grown crystals.

The DC electrical conductivity measurements were carried out to an accuracy of  $\pm 2.5\%$  for all the five grown crystals in the present study, along the c-direction (major growth direction) at various temperatures ranging from 40-100 °C by the conventional two probe method. Temperature was controlled to an accuracy of  $\pm 1$  °C and the observations were made while cooling the sample crystal. Crystals with large surface defect-free were selected and used. The extended portions of the crystal were removed completely and the opposite faces were polished and coated with good quality graphite to obtain a good conductive surface layer. The dimensions of the crystals were measured using a traveling microscope (Least count = 0.001 cm). The DC conductivity ( $\sigma_{dc}$ ) of the crystal was calculated using the relation:

$$\sigma_{dc} = d_{crys} / (R A_{crys}) \quad (1)$$

where R is the measured resistance,  $d_{crys}$  is the thickness of the sample crystal and  $A_{crys}$  is the area of the face of the crystal in contact with the electrode[21]. Plots between  $\ln(\sigma_{dc})$  and  $1000/T$  were found to be vary nearly linear. So the conductivity values can be fitted to the relation:

$$\sigma_{dc} = \sigma_{0DC} \exp \left( -E_{dc} / kT \right) \quad (2)$$

where  $E_{dc}$  is the activation energy, k is the Boltzmann constant, T is the absolute temperature and  $\sigma_{0DC}$  is the parameter depending on the material. Activation energies were estimated using the slopes of the above line plots [ $E_{dc} = -(slope) k \times 1000$ ].

The capacitance ( $C_{crys}$ ) and dielectric loss factor ( $\tan\delta$ ) measurements were carried out to an

accuracy of  $\pm 2\%$  by the parallel plate capacitor method using an LCR meter (Agilent 4284A) for five different frequencies, viz. 100Hz, 1kHz, 10kHz, 100kHz and 1MHz at various temperatures ranging from 40-100 °C along the c-direction in a way similar to that followed by Mahadevan and his co-workers [22, 23]. The required sample crystals were prepared as in the case of DC conductivity measurements. Here also, the observations were made while cooling the sample crystal and the temperature was controlled to an accuracy of  $\pm 1$  °C. The dimensions of the crystals were measured using a traveling microscope (LC = 0.001cm). Air capacitance ( $C_{air}$ ) was also measured. The dielectric constant of the crystal was calculated using the relation

$$\epsilon_r = C_{crys} / C_{air} \quad (3)$$

where  $C_{crys}$  is the capacitance of the crystal and  $C_{air}$  is the capacitance of same dimension of air.

As the crystal area was smaller than the plate area of the cell, parallel capacitance of the portion of the cell not filled with the crystal was taken into account and, consequently, the above equation becomes (Mahadevan's formula [22, 23]),

$$\epsilon_r = [A_{air}/A_{crys}] [[C_{crys} - C_{air} [1-A_{crys}/A_{air}]]C_{air}] \quad (4)$$

where  $C_{crys}$  is the capacitance with crystal (including air),  $C_{air}$  is the capacitance of air and  $A_{air}$  is the area of the electrode. The AC conductivity ( $\sigma_{ac}$ ) was calculated using the relation

$$\sigma_{ac} = \epsilon_0 \epsilon_r \omega \tan\delta \quad (5)$$

where  $\epsilon_0$  is the permittivity of free space ( $8.85 \times 10^{-12} \text{ C}^2 \text{ N}^{-1} \text{ m}^{-2}$ ) and ( $\omega = 2\pi f$ ) is the angular frequency of the applied field. Plots between  $\ln(\sigma_{ac})$  and  $1000/T$  were found to be vary nearly linear. So, the conductivity values can be fitted to the relation

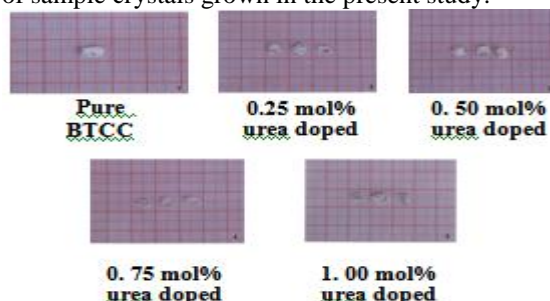
$$\sigma_{ac} = \sigma_{0AC} \exp \left( -E_{ac} / kT \right) \quad (6)$$

where  $E_{ac}$  is the activation energy, k is the Boltzmann constant, T is the absolute temperature and  $\sigma_{0AC}$  is the parameter depending on the material. Activation energies were estimated using the slopes of the above line plots [ $E_{ac} = -(slope) k \times 1000$ ].

### III. Results and Discussion

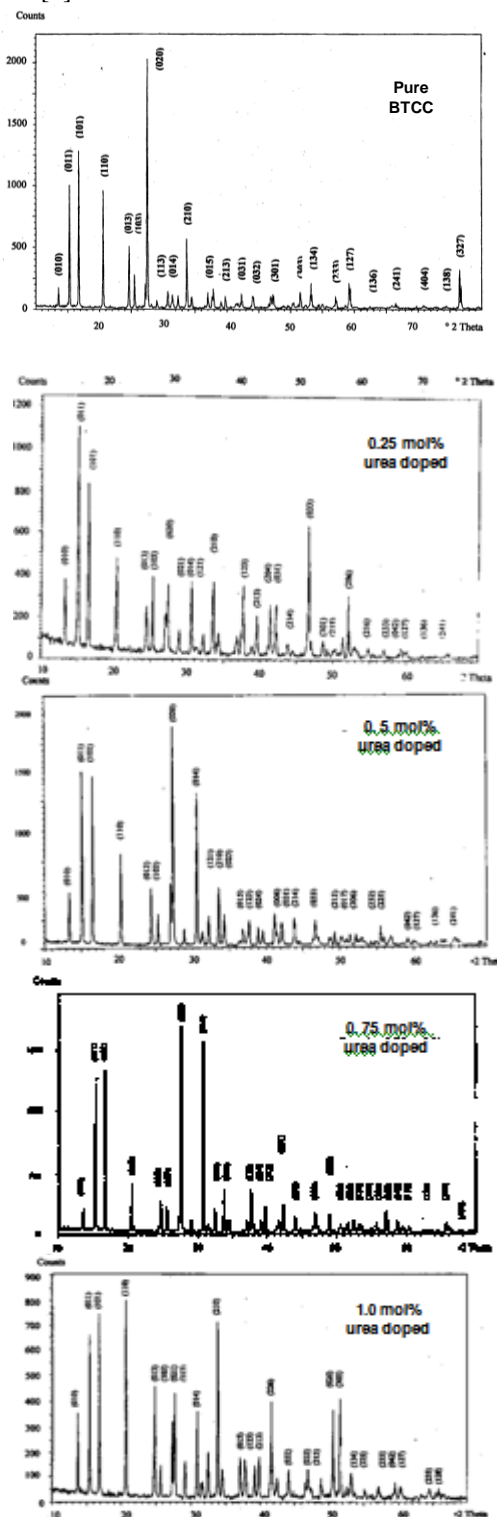
#### 3.1 Single crystals and powder X-ray diffraction analysis

All the five crystals grown are found to be stable and transparent. Figure 1 shows the photographs of sample crystals grown in the present study.



**Fig.1:** Photographs of as grown pure and doped BTCC crystals

Single crystal X-ray diffraction studies reveal that the pure BTCC crystallizes in the orthorhombic crystal system with  $Pmn2_1$  space group and lattice parameters are  $a = 5.815 \text{ \AA}$ ,  $b = 6.431\text{\AA}$ ,  $c = 13.116\text{\AA}$ ,  $\beta = 90^\circ$  C and volume =  $493.0(\text{\AA})^3$ . The lattice parameters and space group obtained agree well with that reported in the literature for the pure BTCC crystal [7].

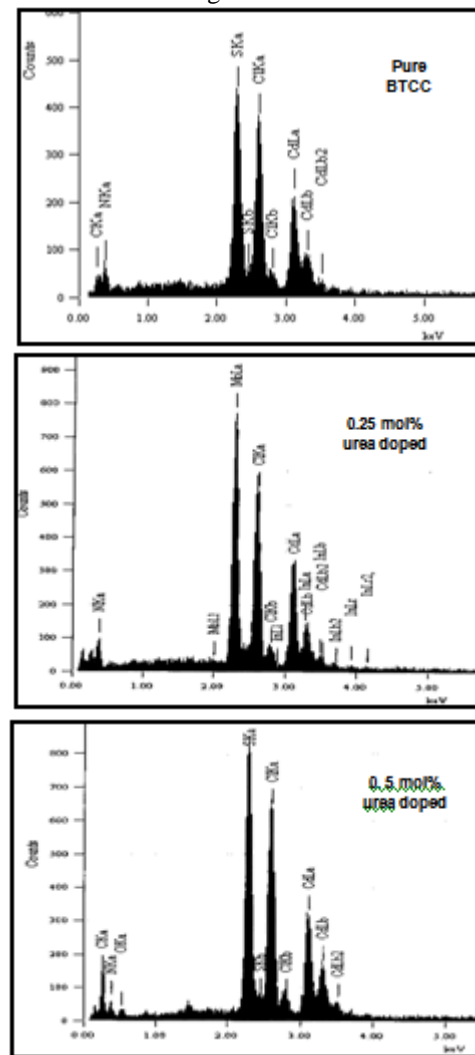


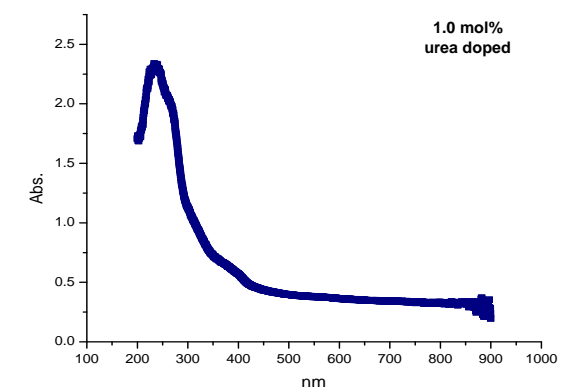
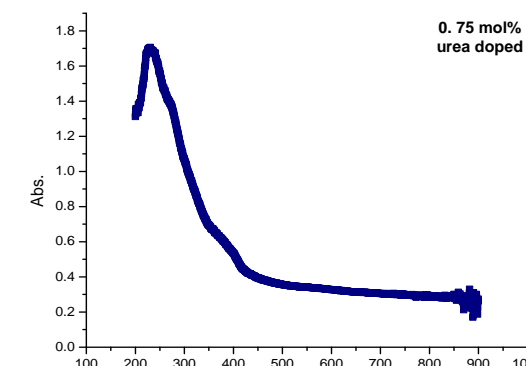
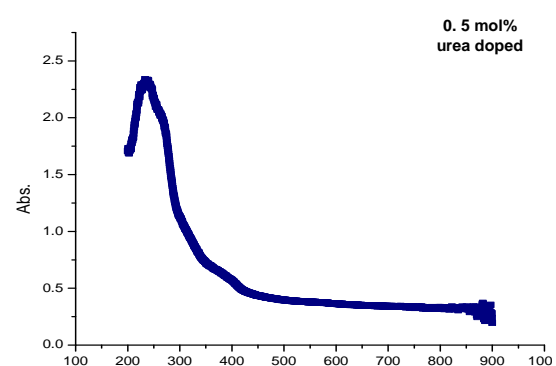
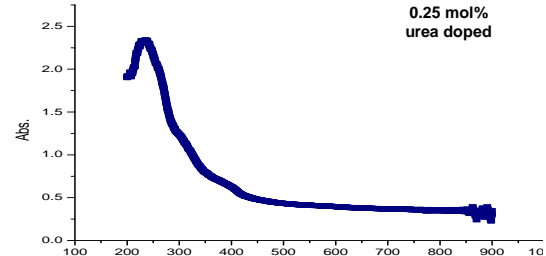
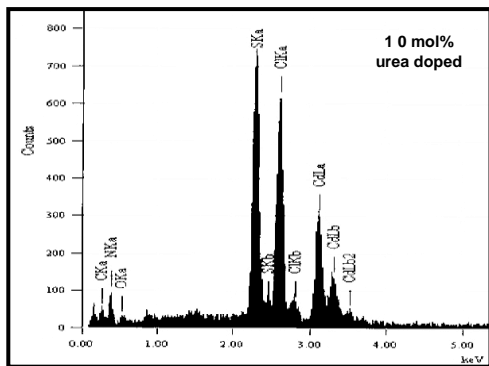
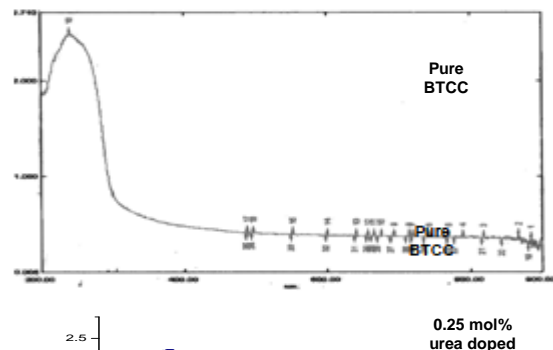
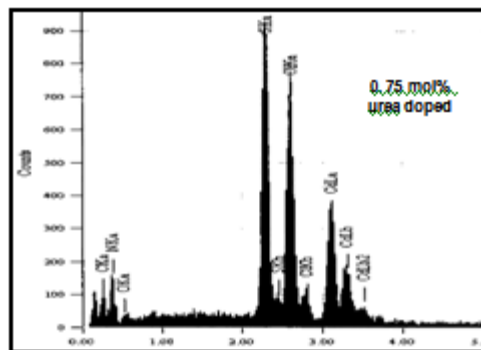
**Fig. 2:** PXRD patterns for the pure and urea doped BTCC crystals (Pure BTCC, 0.25, 0.5, 0.75 and 1.0 mol% urea added)

Figure 2 shows the PXRD patterns of pure and urea doped BTCC crystals. We have found small change in 'd' values of doped BTCC as compared with that of pure BTCC crystal, which may be attributed to the presence of dopants in the BTCC crystal. However, most of the peaks in PXRD patterns resemble with that of the pure BTCC.

### 3.2 Energy dispersive X-ray analysis

The EDAX patterns recorded for the grown crystals are shown in Figure 3.





**Fig.3:** EDAX patterns for the pure and urea doped BTCC crystals (Pure BTCC, 0.25, 0.5, 0.75 and 1.0 mol% urea added)

The oxygen contents obtained through EDAX measurement are provided in Table 1. It can be understood that impurity molecules have entered in to the BTCC host crystal matrix.

**Table 1:** Oxygen contents in urea doped BTCC crystals obtained from the EDAX data

Crystal	Oxygen content from EDAX data	
	Mass %	Atom %
Pure BTCC	-	-
BTCC + 0.25 mol % urea	0.71	1.23
BTCC + 0.50 mol % urea	2.16	2.28
BTCC + 0.75 mol % urea	1.96	2.3
BTCC + 1.0 mol % urea	1.08	1.37

### 3.3 Optical properties

The UV-Vis-NIR absorption spectra observed for pure and urea doped BTCC single crystals are shown in Figure 4.

**Fig. 4:** UV-Vis NIR spectra for the pure and

doped crystals (Pure BTCC, 0.25, 0.5, 0.75 and 1.0 mol% urea added)

The optical absorption spectral analysis is an important study for any NLO material as it can be put into use only if it possesses the required cut off wavelength as well as low optical absorption. For the grown doped crystals absorbance is less than one unit in the entire visible region. The UV cut off wavelength obtained for the grown crystals are entered in Table 2. The UV cut off wavelength for pure BTCC crystal was found to be 300 nm. Thus the cut off wavelength of BTCC can be reduced by doping it with urea. Efficient nonlinear optical crystals are expected to have optical transparency lower cut off wavelengths between 200 and 400 nm [24]. This indicates that the grown doped crystals are efficient NLO crystals which find wide application in electro-optic and second harmonic generation studies.

From the UV cut off wavelength the optical band gap energy for the doped crystals were calculated and also entered in Table 2. The results obtained indicate that urea addition leads to increase in optical band gap energy though not proportionately with the doping concentration used in the solution for the growth of single crystals. However, the trend observed is almost similar to the oxygen content observed in EDAX analysis.

The second harmonic generation (SHG) efficiencies (compared to that of KDP) observed are provided in Table 2. Results obtained indicate that the crystals grown in the present study are NLO active.

**Table 2:** Optical absorption data and SHG efficiencies

Crystal	UV cut off value (nm)	Band gap energy (eV)	SHG efficiency (in KDP unit)
BTCC	300	4.14	7
BTCC + 0.25 mol % urea	275	4.78	6.5
BTCC + 0.50 mol % urea	270	4.87	7.77
BTCC + 0.75 mol % urea	275	4.78	7.22
BTCC + 1.0 mol % urea	295	4.44	9.44

Also, it can be understood that urea addition enhances the SHG efficiency of BTCC crystals.

### 3.4 Electrical properties

Figure 5 shows the variation of DC electrical conductivity ( $\sigma_{dc}$ ) of the grown crystals at temperatures varying from 40-100 °C.

It can be seen that  $\sigma_{dc}$  value increases with the increase in temperature for all the grown crystals. However, no systematic variation is observed with impurity concentration. Except for 0.5 mol% urea doped BTCC crystal, for the other three concentrations, namely, 0.25, 0.75 and 1.0 mol% urea doped, the  $\sigma_{dc}$  value is less than that for pure BTCC crystal.

The electrical conduction in dielectrics is mainly a defect controlled process in the low temperature region. The presence of impurities and vacancies mainly determine this region. The energy needed to form the defect is much larger than the energy needed for its drift. The conductivity of the crystal in the higher temperature region is determined by the intrinsic defects caused by the thermal fluctuations in the crystal [25].

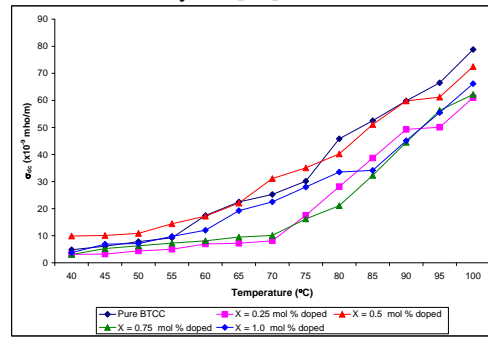


**Fig. 5:** Variation of  $\sigma_{dc}$  with temperature for the pure and urea doped crystals (pure BTCC, 0.25, 0.50, 0.75, 1.00 mol% urea doped)

The conduction region considered in the present study seems to be connected to mobility of vacancies. If the probability of occupation of an interstice is  $\rho$ , then the probability of finding a vacant neighbour site is  $(1-\rho)$ . Even for very high concentrations, of the order of  $10^{20} \text{ cm}^{-3}$ ,  $\rho$  does not exceed  $10^{-2}$  so that in real cases with concentration of interstitials of the order of  $10^{15}$  to  $10^{20} \text{ cm}^{-3}$ ,  $(1-\rho) \approx 1$  [25].

It is also a known fact that urea is a simple organic substance similar to the thiourea present in BTCC. However it is not expected to replace thiourea in the BTCC. So, in addition to occupy the interstitials, the urea molecules are expected to replace  $\text{Cl}^-$  ions to some extent. Moreover, the impurity concentrations considered in the present study are small. Hence the conduction in BTCC is protonic and mainly due to the  $\text{Cl}^-$  ions, the disturbance in the hydrogen bonding system may cause the conductivity to vary nonlinearly with impurity concentration.

The mechanism of electrical conductivity in alkali and silver halide crystals is usually the motion of ions and not the motion of electrons. This has been established by comparing the transport of charge with the transport of mass as measured by the material plated out on electrodes in contact with the crystal [26].

It is assumed that the conductivity of ice is determined by the simultaneous presence of positive

and negative ions and orientational defects – vacant hydrogen bonds (L-defects) and doubly occupied hydrogen bonds (D-defect). Other possible defects are vacancies, and defects associates [27]. The pH value of the initial solution, which determines its ionic composition, can be one of the most important factor that affects crystal conductivity.

From the above knowledge, it is understood that the proton transport depends on the generation of L-defects. Hence the increase of conductivity with the increase in temperature observed for all the crystals grown in the present study can be understood as due to the temperature dependence of the proton transport.

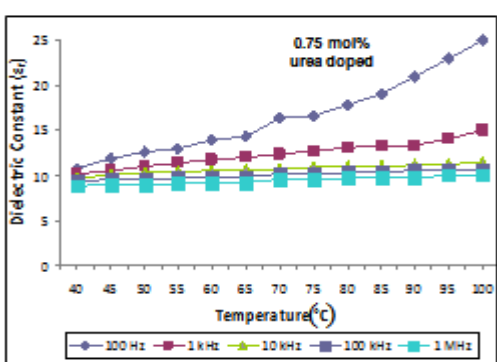
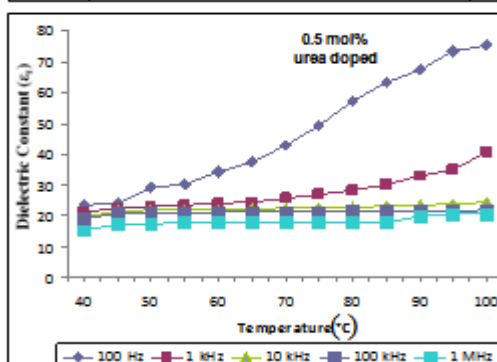
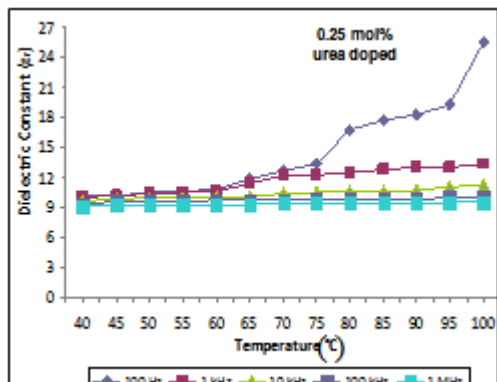
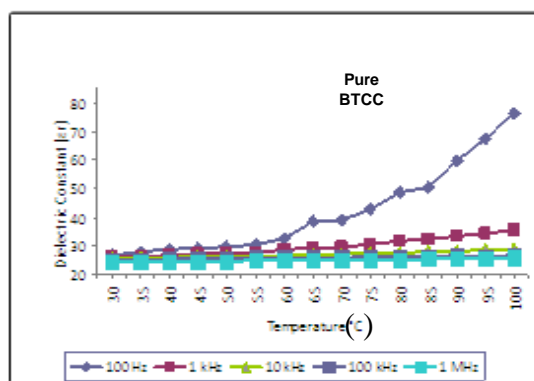
Plots between  $\ln \sigma_{dc}$  and  $1000/T$  (not shown here) are found to be vary nearly linear. So, the DC conductivity values were fitted to the Arrhenius relation. The DC activation energies ( $E_{dc}$ ) were estimated from slopes of the straight line best fitted by least square analysis and are given in Table 3.

**Table 3:** DC & AC activation energies for the pure and urea doped crystals

Crystals	DC activation energy (eV)	AC activation energy (eV)
BTCC	0.308	0.449
BTCC + 0.25 mol % urea	0.499	0.202
BTCC + 0.50 mol % urea	0.480	0.374
BTCC + 0.75 mol % urea	0.501	0.283
BTCC + 1.0 mol % urea	0.354	0.313

The low activation energies observed also suggest that proton transport may be responsible for conduction in the temperature region considered in the present study.

Figure 6 shows the variation of dielectric constant ( $\epsilon_r$ ) with temperature varying from 40-100 °C, for five different frequencies, viz. 100Hz, 1kHz, 10kHz, 100kHz and 1MHz for the pure and urea doped crystals.



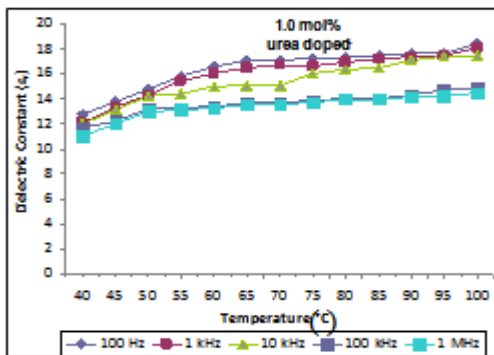


Fig. 6: Variation of dielectric constant with frequency and temperature for pure and urea doped BTCC crystals (Pure BTCC, 0.25, 0.5, 0.75 and 1.0 mol% urea doped)

Variation of dielectric constant with log frequencies for the pure and urea doped crystals for a particular temperature ( $40^{\circ}\text{C}$ ) is shown in Figure 7.

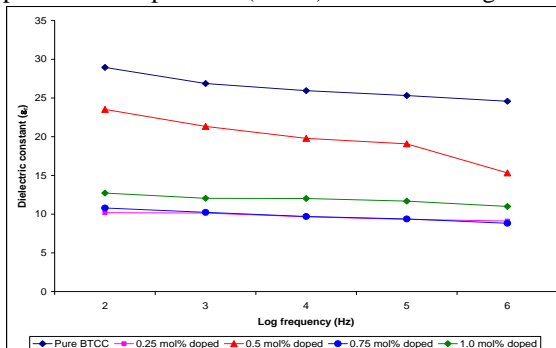


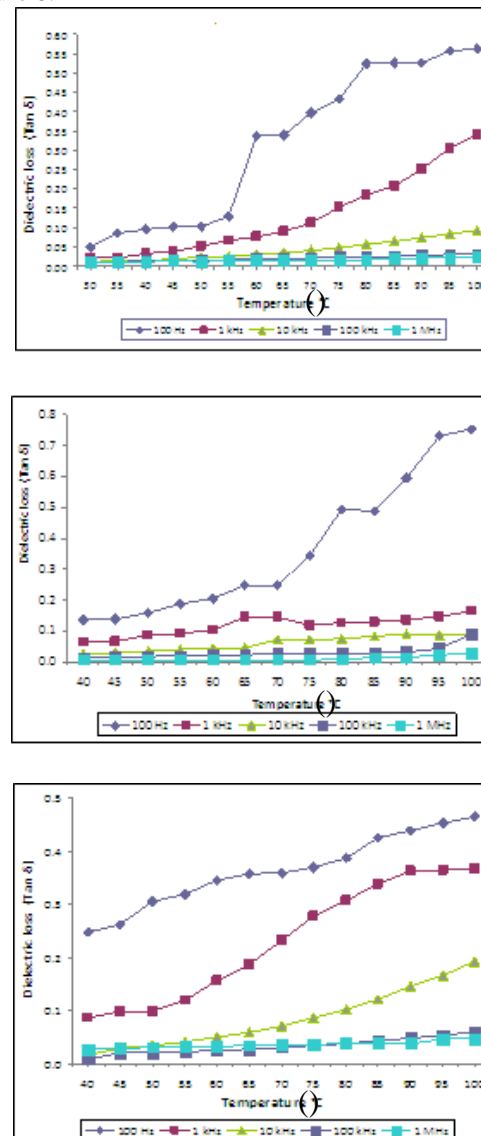
Fig. 7: Variation of dielectric constant  $\epsilon_r$  with log frequency for the pure and urea doped (0.25, 0.5, 0.75 and 1.0 mol%) crystals at  $40^{\circ}\text{C}$

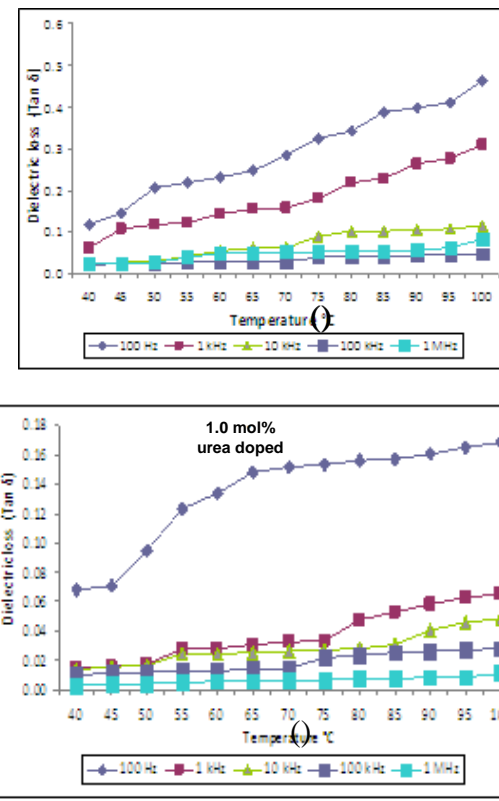
The dielectric constant of a material is generally composed of four types of contributions, viz. ionic, electronic, orientational and space charge polarizations. All these may be active at low frequencies. The nature of variations of dielectric constant with frequency and temperature indicates the type of contributions that are present in them. Variation of  $\epsilon_r$  with temperature is generally attributed to the crystal expansion, the electronic and ionic polarizations and the presence of impurities and crystal defects. The variation at low temperature is mainly due to the expansion and electronic and ionic polarizations. The increase at higher temperatures is mainly attributed to the thermally generated charge carriers and impurity dipoles. Varotsos[28] has shown that the electronic polarizability practically remains constant in the case of ionic crystals. The increase in dielectric constant with temperature is essentially due to the temperature variation of ionic polarizability.

In the present study it has been observed that for all the grown crystals  $\epsilon_r$  value increases with increase in temperature and decreases with increase in frequency. For 0.25, 0.75 and 1.0 mol% urea doped crystals the  $\epsilon_r$  value is found to be less than that for pure BTCC crystal. The  $\epsilon_r$  value for 0.5 mol% urea doped crystal is nearly the same as that for pure BTCC

crystal. Increase in impurity concentration may lead to high density of induced bulk defect states due to competition in getting the interstitial sites for the impurity molecules to occupy. In addition urea molecules are expected to create additional hydrogen bonds. Variation of dielectric constant of BTCC crystals due to urea addition can be attributed to this. Also, the present study indicates, in effect, that the dielectric constant do not vary systematically with impurity concentration which may be attributed to the creation of additional dipoles oriented in random directions due to ionic polarization.

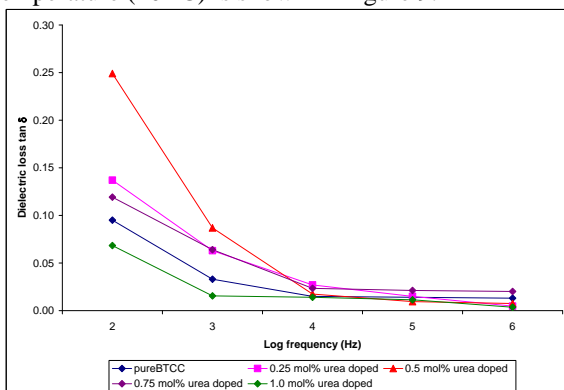
For the grown crystals the variation of dielectric loss factor ( $\tan\delta$ ) with temperature varying from 40-100 °C for five different frequencies viz. 100Hz, 1kHz, 10kHz, 100kHz and 1MHz are shown in Figure 8.





**Fig. 8 :** Variation of dielectric loss with frequency and temperature for pure and urea doped BTCC crystals  
 (Pure BTCC, 0.25, 0.5, 0.75 and 1.0 mol% urea doped)

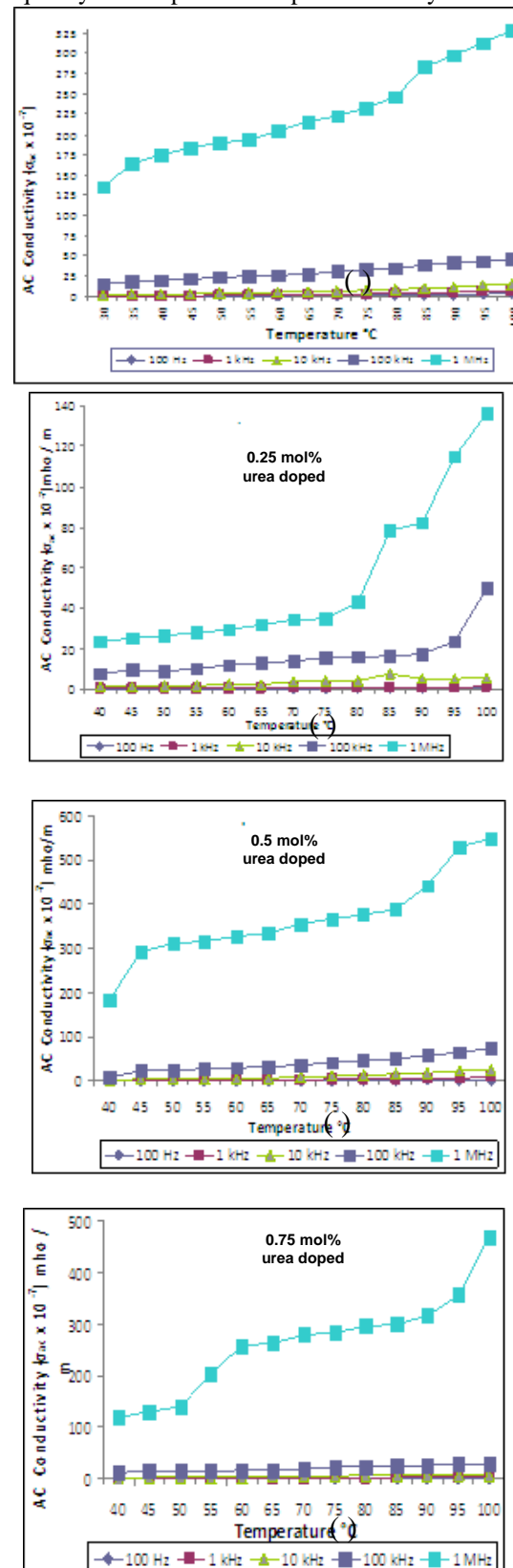
Variation of dielectric loss factor with log frequency for different doped concentrations for the grown crystals corresponding to a particular temperature ( $40^{\circ}\text{C}$ ) is shown in Figure 9.



**Fig. 9 :** Variation of dielectric loss ( $\tan \delta$ ) with log frequency for the pure and urea doped (0.25, 0.5, 0.75 and 1.0 mol%) crystals at 40 °C

Dielectric loss factor is found to increase with increase in temperature for all grown crystals. But its variation with concentration is not systematic. This may be attributed to the complex situation created by the urea molecule in occupying the interstitial sites and by creating additional hydrogen bonds in the crystal structure.

Figure 10 shows the variation of AC electrical conductivity ( $\sigma_{ac}$ ) with temperature and frequency for the pure and doped BTCC crystals.



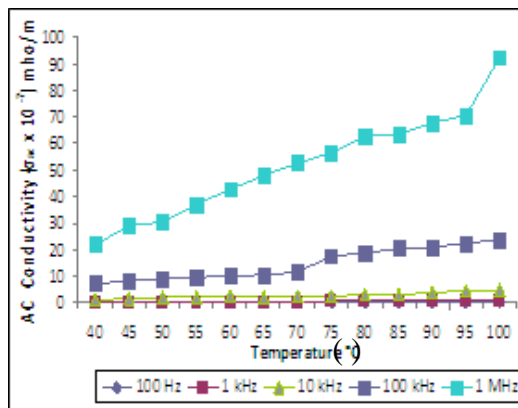


**Fig. 10 :** Variation of AC electrical conductivity with frequency and temperature for pure and urea doped BTCC crystals (Pure BTCC, 0.25, 0.5, 0.75 and 1.0 mol% urea doped)

The AC conductivity of all the grown crystals increases with increase in temperature and frequency. When the temperature of the crystal is increased, there is a possibility of weakening of hydrogen bond. This results in an enhanced conductivity in these materials. The increase of conductivity with the increase in temperature observed in the present study is similar to that observed for some tartrate crystals [29]. When the temperature of the crystal is increased, there is a possibility of weakening of hydrogen bond due to rotation of the tartrate ion. This results in an enhanced conduction in these materials. The variation of  $\sigma_{ac}$  with temperature and impurity concentration is similar to the variation of dielectric constant.

Figure 11 shows the variation of AC electrical conductivity  $\sigma_{ac}$  with log frequency for different doped concentrations, corresponding to a particular temperature [40 °C]. The  $\sigma_{ac}$  values are observed to be more than  $\sigma_{dc}$  in all the grown crystals which is a normally expected behavior for a dielectric material.

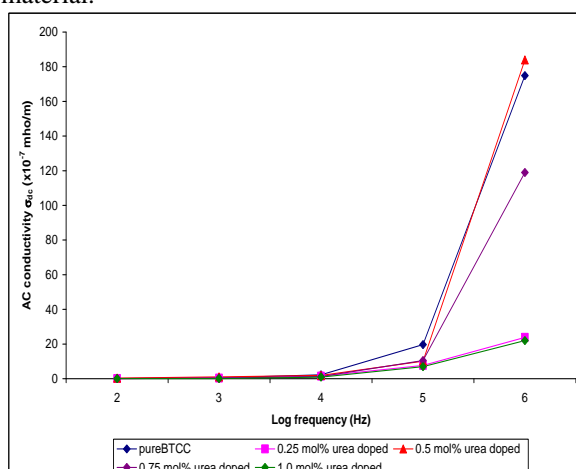


**Fig. 11:** Variation of AC electrical conductivity ( $\sigma_{ac}$ ) with log frequency for the pure and urea doped (0.25, 0.5, 0.75 and 1.0 mol%) crystals at 40 °C

Plots between  $\sigma_{ac}$  and  $1000/T$  are found to be vary nearly linear (not shown here). Using the graph AC activation energies were calculated and given in Table 3. For the doped crystals the AC activation energy is found to be less than DC activation energy. This is an expected behavior only. The low activation energies observed suggest that protonic movement may be responsible for conduction in the temperature region considered in the present study.

#### IV. Conclusions

Single crystals of BTCC added with urea were grown by the free evaporation method and characterized structurally, optically and electrically. The PXRD patterns showed slight variation in '2θ' values due to the incorporation of dopant. The optical absorption spectral studies confirm that the doped crystals have absorbance less than one unit in the entire visible region, and lower UV cut off wavelengths compared to pure BTCC crystals. Thus the organic dopant urea plays a key role in improving the optical quality of BTCC crystals and is likely to enhance the NLO property. Analysis of the DC and AC electrical conductivity data indicates that urea addition leads to random orientation of hydrogen bonds and consequently the nonlinear variation of  $\sigma_{dc}$  and  $\sigma_{ac}$  with impurity concentration. The present study, in effect, indicates that doping BTCC with urea leads to the discovery of new BTCC crystals with tuned optical and electrical properties useful for the construction of opto-electronic and photonic devices.

#### V. Acknowledgement

One of the authors (I.S. Prameela Kumari) thanks University Grant Commission (UGC) for granting Faculty Development Program (FDP) award.

#### References

- [1] M.H. Jiang and Q. Fang, *Adv. Mater.*, **11**, 1999, 1147.
- [2] K. Nagarajan, *Cryst. Res. Technol.*, **39**, 2004, 414.
- [3] J. Ramajothi, S. Dhanuskodi and K. Nagarajan, *Cryst. Res. Technol.*, **39**, 2004, 414.
- [4] V. Venkataraman, C.K. Subramanian and H.L. Bhat, *J. Appl. Phys.*, **11**, 1995, 6049.
- [5] V. Venkataraman, H.L. Bhat, M.R. Srinivasan, P. Ayyub and M.S. Multani, *J. Raman Spectrosc.*, **28**, 1997, 779.
- [6] V. Venkataraman, S. Maheswaran, J.N. Sherwood and H.L. Bhat, *J. Cryst. Growth.*, **179**, 1997, 605.
- [7] P.M. Ushasree, R. Muralidharan, R. Jayavel and P. Ramasamy, *J. Cryst. Growth.*, **218**, 2000, 365.
- [8] P.M. Ushasree and R. Jayavel, *Optical Materials*, **21**, 2002, 599.

- [9] J. Pricilla Jeyakumari, J. Ramajothi and S. Dhanusskodi, *J. Cryst. Growth.*, 269, 2004, 558.
- [10] S. Selvakumar, J. Packiam Julius, S.A. Rajasekharan A. Ramanand and P. Sagayaraj, *Mater. Chem. Phys.* 89, 2005, 244.
- [11] S. Selvakumar, S.A. Rajasekar, K. Thamizharasan, S. Srivanesan, A. Ramanand and P. Sagayaraj, *Mater. Chem. Phys.*, 93, 2005, 356.
- [12] S. Arivonnammal, R. Selva Vennila, S. Radhika and S. Arumugam, *Cryst. Res. Technol.*, 40, 2005, 896.
- [13] S. Ravi and P. Subramanian, *Solid State Sciences.*, 9, 2007, 961.
- [14] R. Uthrakumar, C. Vesta, C. Jusin Raj, S. Dinakaran, Rani Christu Dhas and S. Jerome Das, *Crys. Res. Technol.*, 43, 2008, 428.
- [15] N.R. Dhumane, S.S. Hussaini, V.G. Dongre, P.P. Karmuse and M.D. Shirsat, *Crys. Res. Technol.*, 44, 2008, 269.
- [16] J.J. Jang, S.J. Luo, L. Yi and A. Laref, *Physica B. Condensed Matter.*, 408, 2013, 175.
- [17] M. Senthilkumar and C. Ramachandraraja, *Optik-International Journal for Light and Electron Optics.*, 124, 2013, 1269.
- [18] P.M. Ushasree, R. Jayavel and P. Ramaswamy, *Mater. Sci. Eng.*, B65, 1999, 153.
- [19] H. Lipson and H. Steeple, *Interpretation of X-ray Powder Diffraction Patterns*, (MacMillian, New York, 1970).
- [20] S.K. Kurtz and T.T. Perry, *J. Appl. Phys.*, 39, 1968, 3798.
- [21] A. Anne Assencia and C. Mahadevan, *Bull. Mater. Sci.*, 28, 2005, 415.
- [22] S. Goma, C.M. Padma and C.K. Mahadevan, *Mater. Lett.*, 60, 2006, 3701.
- [23] M. Priya and C.K. Mahadevan, *Physica B* 403, 2008, 67.
- [24] Y.L. Fur, R. Masse, M.Z. Cherkaoui and J.K. Nicoud, *Z. Kristallogr.*, 210, 1975, 856.
- [25] J. Bunget and M. Popescu, *Physics of Solid Dielectrics* (Elsevier, New York, 1984)
- [26] C. Kittel, *Introduction to Solid State Physics* (7<sup>th</sup> edn) (John Wiley and Sons, Singapore, 2005)
- [27] L.B. Harris and G.J. Vella, *J. Chem. Phys.*, 58, 1973, 4550.
- [28] P. Varotsos, *J. Phys. Lett.* 39, 1978, L79.
- [29] L.B. Harris and G.J. Vella, *J. Chem. Phys.*, 58, 1973, 4550.